Discontinuous jamming transitions in soft materials: coexistence of flowing and jammed states

2008 J. Phys.: Condens. Matter 20 283103

(http://iopscience.iop.org/0953-8984/20/28/283103)

IOP PUBLISHING JOURNAL OF PHYSICS: CONDENSED MATTER

J. Phys.: Condens. Matter **20** (2008) 283103 (14pp) doi:10.1088/0953-8984/20/28/283103

TOPICAL REVIEW

Discontinuous jamming transitions in soft materials: coexistence of flowing and jammed states

Michael Dennin

University of California, Irvine, CA 92697-4575, USA

E-mail: mdennin@uci.edu

Received 10 January 2008, in final form 24 May 2008
Published 13 June 2008
Online at stacks.iop.org/JPhysCM/20/283103

Abstract

Many systems in nature exhibit transitions between fluid-like states and solid-like states, or 'jamming transitions'. There is a strong theoretical foundation for understanding equilibrium phase transitions that involve solidification, or jamming. Other jamming transitions, such as the glass transition, are less well understood. The jamming phase diagram has been proposed to unify the description of equilibrium phase transitions, the glass transitions, and other nonequilibrium jamming transitions. As with equilibrium phase transitions, which can either be first order (discontinuous in a relevant order parameter) or second order (continuous), one would expect that generalized jamming transitions can be continuous or discontinuous. In studies of flow in complex fluids, there is a wide range of evidence for *discontinuous* transitions, mostly in the context of shear localization, or shear banding. In this paper, I review the experimental evidence for discontinuous transitions. I focus on systems in which there is a discontinuity in the rate of strain between two, coexisting states: one in which the material is flowing and the other in which it is solid-like.

(Some figures in this article are in colour only in the electronic version)

Contents

1. Introduction

Most people are familiar with the everyday phenomenon of 'jamming' as a function of density. This is especially true for people who drive in heavily populated areas. As the density of cars on the road increases, the system makes a transition from a flowing state (traffic moving) to a jammed state (cars at a stand-still). An interesting feature of jamming is its ubiquitous occurrence in nature. One observes transitions from freely flowing behavior to jammed behavior in all types of systems under a wide range of control parameters. Perhaps the first such transition that students learn about formally is the freezing of a fluid as a function of decreasing temperature. Eventually, one also studies freezing as a function of increasing density. For these familiar transitions, one is working in the realm of equilibrium transitions. Significantly less well understood are jamming transitions as a function of applied stress [1, 2].

Such transitions are interesting because they are examples of nonequilibrium transitions. In contrast to equilibrium transitions, there is no general theory of nonequilibrium jamming transitions at this time [3]. One of the goals of studies of jamming transitions is to understand how useful the tools and ideas used for equilibrium systems might be for understanding the nonequilibrium case.

This concept was expressed by Liu and Nagel when they proposed that a generalized jamming phase diagram [2] was a useful concept for the characterization of a wide range of phenomena. The basic idea is that there exists a unified description of jamming based on considering the behavior of systems as a function of temperature, the inverse of density, and applied stress (or load). In this picture, equilibrium systems exist in the temperature–inverse density plane. In the language of equilibrium phase transitions, a continuous jamming transition is a second order phase transition and a discontinuous jamming transition is a first order phase transition. A major question is whether or not the characterization of transitions as *continuous* or *discontinuous* remains useful for the nonequilibrium jamming transitions. In the generalized jamming picture, many complex fluid systems are effectively at zero temperature because of the large energies associated with motions of the constituent elements of the materials. For example, in typical granular materials, the thermal motion of the individual grains of sand can be ignored. One goal of the jamming phase diagram is to provide a mapping between jamming transitions that occur in the different planes. For example, if one can map the stress axis to the temperature axis, then elements of our understanding of equilibrium jamming transitions as a function of temperature can be applied to nonequilibrium transitions as a function of applied stress.

Before discussing some of the specific models that have been used in the study of the jamming transition, it is worth defining some of the terms in more detail. The jamming transition is fundamentally a transition from a fluid-like state to a solid-like state (the reverse transition is often referred to as unjamming). Though this transition is relatively intuitive, it is important to define each of the states. Because the systems of interest cover materials ranging from amorphous molecular systems (such as common window glass) to complex fluids such as foams and granular matter, a definition based on molecular characteristics is not useful. Instead, one defines the state of the material based on mechanical properties. In this case, the two most common properties to measure are the elastic shear modulus and the viscosity.

Recall that a stress, σ, is a force per area applied to the surface of a material. The shear stress is a force applied parallel to the surface. A fundamental difference between solids and fluids is the response to shear stresses. Fluids cannot support shear stresses, so they flow in response to an applied shear stress. Solids can support shear stresses, so they deform, but do not flow, in response to an applied shear stress. To describe these different types of mechanical response, one uses the shear strain γ, which is the dimensionless displacement of the material, and the rate of strain $\dot{\gamma}$, which is the time derivative of strain. Therefore, one can define the effective viscosity η as the shear stress divided by the rate of strain and the elastic shear modulus as the shear stress divided by the strain. Typically, as one approaches the jamming transition from the fluid phase, the viscosity is found to diverge (as a larger stress is required to cause the material to flow at the same rate of strain), and at the transition, the material develops a non-zero elastic modulus. (For the rest of the paper, unless specified the elastic modulus will refer to the elastic shear modulus.) Likewise, if one starts in the solid state and approaches the unjamming point, the elastic modulus goes to zero at the transition point, and the system begins to flow. Depending on the details of measuring the transition, there can be additional considerations. For a more detailed discussion of the mechanical response of materials, there are a number of good text books and references [4].

The purpose of this review is to focus on the experimental evidence for a specific class of jamming transitions: discontinuous transitions. Therefore, a detailed review of the theoretical efforts in the area of jamming, and even the experimental studies of continuous jamming transitions is beyond the scope of this paper. More complete overviews of the general jamming transition exist [3]. However, it is worth commenting on some common elements of models of jamming transitions to set the context for our discussion of the discontinuous jamming transition.

Most models of jamming focus on the interplay between heterogeneities in the material and the mechanical response. Three examples of this will be described briefly. These have been selected merely to illustrate some of the common elements, and it is important to realize that there are a broad class of models that can describe the jamming/unjamming of various materials.

One of the first discussions to use the language of jamming involved the application of the concept of force chains (the heterogeneity of interest in this model) in colloidal and granular systems to the phenomenon of jamming [1]. The basic idea is that under an applied load, materials would develop force chains that could support a specific class of loads elastically. However, because of the heterogeneous nature of the chains, if a different load was applied (for example, along a different axis) the chains would not support the load and the material would deform plastically. Thus, the material was described as *fragile*.

Another model of materials that experience jamming is *soft glassy rheology* [5, 6]. Basically, this describes a large class of materials in terms of local elastic regions with a distribution of yield stresses (again, a spatial heterogeneity in the material). The yield stress is the value of stress at which an elastic region undergoes plastic deformation or flow. The regions are subject to activated dynamics that are controlled by an effective temperature, which is related to the applied rate of strain.

The first two models were introduced in the context of complex fluids, such as colloids, granular matter, and foams. An example of a model first applied to molecular systems is the concept of shear-transformation zones (STZ) [7]. STZ models have been used with a high degree of success in describing molecular plasticity. These are based on the concept of local

regions of bistability in a material. The transition between two different local configurations of particles provides the fundamental source of plasticity, and hence, unjamming. In particular, it is noteworthy that this model is applicable in the limit of no underlying stochastic fluctuations and therefore works even at zero temperature.

Finally, one of the first experimental confirmations that the jamming phase diagram is a useful concept was reported in [8]. This work used three different colloidal systems to measure jamming transitions as a function of all three parameters: density, temperature, and applied stress. The transition was determined by measuring the divergence in the viscosity of the material or the location at which the elastic modulus of the material became non-zero. In the context of this review, it is important to note the transitions in this case were all continuous, as opposed to the discontinuous transitions reviewed in this review.

1.1. Continuous versus discontinuous transitions

In order to distinguish between a continuous and a discontinuous jamming transition, it is important to understand the two basic classes of experiments: constant applied stress and constant applied rate of strain. As discussed, one of the expected control parameters for the jamming transition is the applied stress. Therefore, constant stress experiments provide the most direct probe of the transition. (While the stress across a material can fluctuate spatially and temporally during flow, by constant stress, we are referring to the average stress over a large enough volume to be well defined.) Below a critical stress, the system is jammed; no flow occurs; and one measures a non-zero elastic modulus. Above a critical stress, flow is initiated, and one measures a finite viscosity. The transition can be continuous or discontinuous, but what does this mean?

First, recall the classic first order equilibrium phase transition with a discontinuity in density—freezing/melting. In this case, a classic measurement is to fix the pressure and vary the temperature. At the transition temperature, one measures a discontinuous change in the density of the material. If one sits exactly at the transition temperature, one can observe the coexistence of the two phases. This is often done in the context of fixing the temperature and varying the volume of the system. In this case, the pressure of the system is measured. Typically, as one decreases the volume, the pressure increases until the transition is reached. At this point, one continues to decrease the *average* density, but the measured pressure stays constant. Locally, the system phase separates into either the solid or liquid state, and the average density is a measure of the relative proportion of one phase to the other (see figure 1).

What is the analog for constant stress or constant rate of strain experiments as a probe of the jamming transition? In this case, the stress is analogous to the temperature or pressure, and the rate of strain is analogous to the density. For experiments in which the stress is varied, the relevant question is whether or not the rate of strain increases continuously from zero as the stress is increased above the critical stress or if there is a discontinuous jump in the rate of strain. Therefore, in some sense this is the most straightforward method for probing the

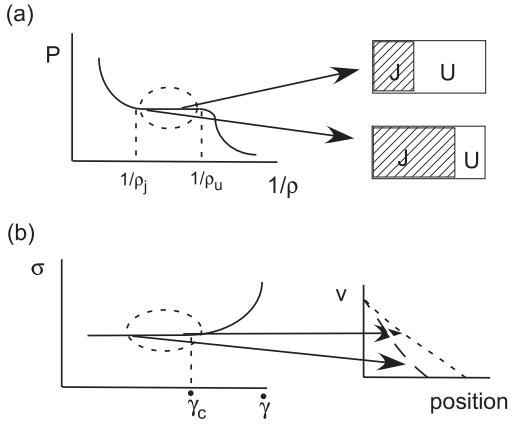

Figure 1. This figure provide a schematic illustration of the analogy between a first order phase transition (a) and a discontinuous jamming transition (b). In (a), the behavior of the system as the density is varied is illustrated. In particular, the coexistence region for which the pressure remains constant is highlighted. The figures on the right schematically illustrate the system separating into two regions: one with the jammed (J), or solid, phase and one with the unjammed (U), or fluid phase. In (b), the analogous behavior is illustrated for the jamming transition as the applied rate of strain ($\dot{\gamma}$) is varied. In this case, the figures on the right illustrate the system being divided into two regions: one of flow (non-zero velocity) and no-flow (zero velocity). In this case, because there is a critical rate of strain, the slope of the velocity as a function of position curve is non-zero at the point where the velocity goes to zero. This indicates the discontinuous nature of the transition.

continuity of the jamming transition. For the case of constant rate of strain experiments, the analogy is to the constant temperature experiments in which average density is varied. This is a very common experimental technique for rheological measurements in either Couette rheometers or cone and plate rheometers.

The basic idea for constant rate of strain experiments is the same for either Couette or cone and plate rheometers. For the Couette case, a material is confined between two concentric cylinders. For the cone and plate, the material is confined between a cone and plate. Then, one of the confining surfaces is moved at a constant velocity, applying a constant rate of strain to the system. (Note: in this case, *constant rate of strain* refers strictly to the dependence in time. Depending on the parameters of the specific system, the rate of strain may vary in space.) The stress on one of the walls is then measured—either the stress required to maintain the constant rotation of the moving wall or the stress required to hold the other wall fixed—and from the measured stress/rate of strain relation, the mechanical properties are determined.

When studying the jamming transition using constant rate of strain, one can consider both the initial transient response of the system and the steady-state properties. If the density is sufficiently low, the system flows immediately, and the stress immediately jumps to a non-zero value. This corresponds to an unjammed state. In contrast, if the system is jammed, one observes an elastic response initially, and the stress increases linearly with the strain. In this case, the critical stress for unjamming is eventually reached. At this point, all, or some, of the system begins to flow. The steady-state behavior depends

on the relation between the average rate of strain and the critical rate of strain. If the applied rate of strain is sufficiently low, one observes the coexistence of a flowing and non-flowing region in the system. This is often referred to as shear localization, flow localization, or shear banding. From the perspective of this review, an important question is whether or not the rate of strain is continuous across the boundary from flow to non-flow. A discontinuity in the rate of strain would be a signature of a discontinuous jamming transition. As with our analogy to density in equilibrium transitions, one expects the size of the regions of flow and non-flow to be set by the average applied rate of strain. This is illustrated schematically in figure 1.

1.2. Constitutive relations

Another issue that is worth addressing briefly in the introduction is the connection between the jamming/phase transition picture and 'traditional' explanations of shear banding for yield stress fluids. Yield stress fluids are ones that below a critical stress do not flow, and above a critical stress, they flow. At the most basic level, this behavior is natural to discuss in the context of the jamming phase diagram, in which the yield stress corresponds to the unjamming transition.

Traditionally, yield stress materials are described in terms of various *constitutive* relations. A constitutive relation typically is given in terms of the stress (σ) as a function of the strain (γ) and/or the rate of strain ($\dot{\gamma}$). This function is used in Cauchy's equation to derive the deformation or flow field for the material. A standard example for yield stress materials is the Herschel–Bulkley model: $\sigma = \sigma_y + \eta\dot{\gamma}^n$ if $\sigma \geqslant \sigma_y$. In this expression, σ_y is the yield stress. Below σ_y, one can either treat the system as infinitely rigid (a solid body) or as having a finite elastic modulus and no viscosity. A key feature of the Herschel–Bulkley model is the treatment of the material as having a *single* constitutive relation: $\sigma = \sigma_y + \eta\dot{\gamma}^n$. Because of this, the rate of strain is always continuous in the material. How does this differ from the jamming picture? Though in practice, especially for continuous jamming transitions, one might use standard rheological relations to describe the mechanical response of the system, the jamming picture focuses on the transition in the material between two distinct phases. As we outlined briefly, many of the models focus on specific structural changes in the material. When approaching discontinuous transitions, this provides a useful guide for developing new rheological models.

It is worth commenting on the fact that the concept of yield stress itself is not completely well defined, and there exist various practical definitions of the yield stress. For a good review of the current understanding of yielding behavior, see [9]. Given this situation, the jamming transition paradigm, by approaching the question from a different point of view, might provide insights into our understanding of the specific case of yield stress materials.

1.3. Structure of the paper

There are a number of experimental systems for which discontinuous transitions have been observed using a constant rate of strain. For some of these, important confirmation of the discontinuity has been achieved with constant stress experiments. In this review, I will discuss a number of these and their relationship to each other. In terms of the jamming transition, the important case is the coexistence of a flowing state with no-flow, and that will be the focus of this review. But, for comparison, I will also briefly discuss cases of coexistence of two different flow regimes. The focus of this review is the experimental results. The systems that will be discussed are described briefly in section 2, and the experimental results in section 3. However, it is useful to put these results in the context of proposed mechanisms for understanding the observed discontinuities in the rate of strain. This will be done in section 4.

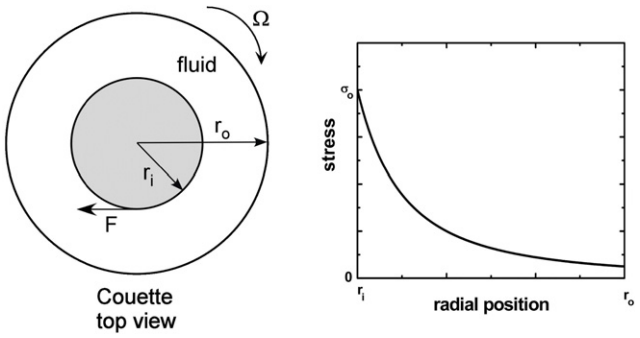

Figure 2. Schematic drawing of a Couette viscometer (left side of panel) and an illustration of the radial stress dependence (right side of the panel). An important feature of Couette flow is the $1/r^2$ dependence of the stress.

2. Experimental systems

In this paper, I review the results from a number of experimental systems that exhibit a discontinuous transition from flow to no-flow. There are two aspects of the work that are important to consider: (1) the experimental techniques used to study the system and (2) the details of the system itself. Both of these aspects play an important role, and it is useful to discuss them separately. I will first describe the basic experimental techniques. This will include essential aspects of the method used to generate the flow, the pros and cons of the methods, and the methods used to measure the velocity profile (the key measurement in all of these studies). After reviewing the experimental techniques, I will discuss the systems that were used for the studies. In this section, I will discuss the main two-dimensional system used, bubble rafts, and a number of three-dimensional materials. This will provide a relatively comprehensive review of both the various techniques used to probe the discontinuous jamming transition and the materials for which it is has been observed.

2.1. Experimental methods

There are three standard geometries that have been used to study shear localization in complex fluids: Couette flow (figure 2), cone and plate (figure 3), and oscillatory planar

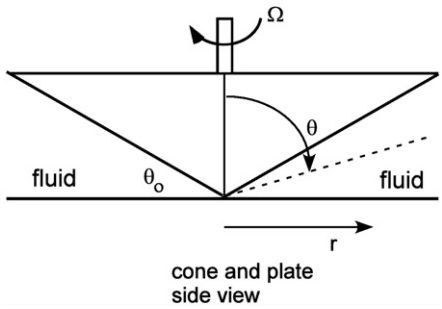

Figure 3. Schematic drawings of a cone and plate viscometer. In standard usage, the angle for the cone (θ_o) is sufficiently small that the stress as a function of radial position is uniform.

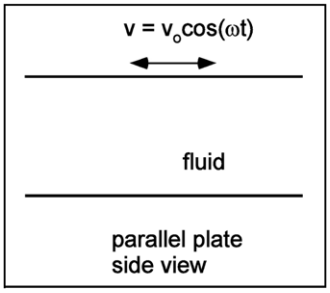

Figure 4. Schematic drawing of oscillatory parallel plate geometry. In this case, the stress is uniform as a function of distance from a plate. However, the phase of the stress relative to the driving of the oscillating plate provides information on the viscoelastic nature of the material.

flow (figure 4). I will discuss each of these in enough detail to illustrate how the measurements complement each other.

Couette flow consists of the flow between two concentric cylinders. This is a standard geometry for making rheological measurements. The basic measurement in this geometry consists of measuring the stress as a function of the rotation rate of one of the two cylinders. Figure 2 illustrates the case of rotating the outer cylinder. An advantage of this system is the fact that it is extremely well characterized. One knows analytically the velocity profile in the system for many classes of fluids, even some that are non-Newtonian. In the cases of interest, the velocity is purely azimuthal (around the inner cylinder) and only a function of the radial position between the cylinders ($v_\theta(r)$). However, one should be aware that various conventions exist in the literature for scaling the measured velocity.

In the case of rotating the outer cylinder with rotation rate Ω, an elastic material (or jammed state) will exhibit rigid body motion with $v_\theta(r) = \Omega r$. Therefore, when the outer cylinder is rotated, it is conventional to report velocities normalized by Ωr, with $v(r) = v_\theta(r)/\Omega r$. In this case, $v(r) = 1$ corresponds to rigid body rotation, which is equivalent to no-flow. This is a critical point. In the context of jamming, a jammed material can still 'move', just as any solid can spin about its axis. What is relevant for unjamming is the existence of 'flow', which exhibits viscous dissipation. Another way to describe this is that flow requires a non-zero rate of strain. When the inner cylinder is rotated, $v(r) = v_\theta(r)$, and $v(r) = 0$ corresponds to no-flow. In some cases, for rotation of the inner cylinder, the velocity is scaled by the velocity at the inner cylinder, so that the maximum velocity is 1.

An important feature of Couette flow is the fact that there exists a radial variation in the stress. This is illustrated in figure 2. This is minimized in the case of narrow gap Couette viscometers, but often plays a role in measurements with complex fluids. The radial variation of the stress is a direct consequence of the balance of torques in steady-state flows. Consider a Couette device with cylinders of length L and inner and outer radii r_i and r_o, respectively. By definition, the torque per unit length, T/L, on a surface of a cylindrical slice at position r is related to the tangential force per unit length F/L by $T/L = rF/L$. (For example, in figure 2, the tangential force on the inner cylinder is indicated.) The tangential force is related to the shear stress σ by $F/L = (2\pi r L\sigma)/L$, where the definition of stress as force per area is used. Combining these two relations gives the stress as a function of radial position: $\sigma(r) = (T/2\pi L)(1/r^2)$. Therefore, we see that the stress exhibits a $1/r^2$ dependence on the radius. Notice, this result is based only on the balance of torques, and it is independent of whether or not the outer or inner cylinder is rotated [10].

The variation of stress in the Couette geometry is important when comparing different experiments which use Couette flow but rotate different cylinders. Though the variation of stress plays a role in the initial observations of the shear localization, if not treated carefully, it can add a layer of confusion to the interpretation of the observed shear banding in complex fluids. This is especially true for the case of a continuous jamming transition. In this case, it is likely that there would be essentially no feature in the velocity profile that would distinguish between the coexistence of two phases and a single constitutive equation for the material. In contrast, for the work reviewed here, the drawbacks of the Couette geometry are minimized precisely because the system exhibits a discontinuous transition. The existence of the discontinuity in the rate of strain is a clear signal that would not exist for standard rheological models.

The other standard rheometer that is used in these studies is a cone and plate rheometer. One confines the fluid between a plate and a cone that has a relatively shallow angle (θ_o sufficiently small that $\sin\theta_o \approx \theta_o$). This results in a constant stress across the system, to a very good approximation. Also, the rate of strain is constant, given by $\dot{\gamma} = -\Omega/\theta_o$. Therefore, the cone and plate geometry provides unambiguous measures of the dependence of the jamming transition on the applied rate of strain, and removes potential complications due to spatial variations in stress. This geometry is not applicable to the two-dimensional systems.

The final geometry I consider is the flow between two oscillating parallel plates (see figure 4). This geometry has a constant stress across the gap, without any approximations. This plays a key role in unambiguously establishing the coexistence of two different states of the material, especially at a constant value of the stress. Another useful feature of an oscillatory geometry is the ability to consider both the frequency response of the material and to provide clear tests of

the linearity of the response. When applying a sinusoidal drive to the system, a linear material will have a sinusoidal response. Additionally, a perfectly elastic material will have a stress that is in-phase with the strain, and a perfectly viscous material will have a stress that is $\pi/2$ out-of-phase. This is usually reflected by referring to a complex shear modulus, $G^* = G' + iG''$. Then, for an oscillatory applied strain, $\gamma = \gamma_o e^{i\omega t}$, the stress is given by $\sigma(\omega) = (G' + iG'')\gamma$. Here G' represents the in-phase, or elastic, response, and G'' represents the out-of-phase, or viscous, response. Therefore, if one can measure the stress in response to an applied strain (or vice versa) one can simultaneously probe both the viscous and elastic response of the material.

A final comment on the various techniques used in studying complex fluids. In all cases, it is critical to understand the role of wall-slip. Solutions to this problem range from simply measuring the degree of slip at the wall (for example, [11]) to using various techniques to roughen the walls to ensure that no slip occurs (for example, [12]).

2.2. Materials

The specific systems discussed in this review are all examples of complex fluids. Here, the term complex fluid is used to refer to materials that are comprised of the coexistence of two or more phases or materials, such as foams, colloids, emulsions, slurries, pastes, and granular materials. Foams are gas bubbles (the 'particle') with liquid walls, and colloids are solid particles (the 'particle') in a fluid [13]. A key parameter is the volume fraction of the 'particle'. For the foam, this is the gas volume fraction. The limit of a volume fraction of 1 is a perfectly dry foam. This is an idealization with infinitely thin walls. For all of these systems, there is a jamming/unjamming transition as a function of the volume fraction (or density) of the particles. This is not the focus of this review, but roughly speaking, as the system increases the density of particles, there is a jamming transition around random close packing [14].

Above this jamming transition, one can refer to the materials as either in the 'wet' limit or the 'dry' limit. I have adopted this language from the case of foams, for which it refers to the fraction of fluid in the foam. In the wet limit, the bubbles are approximately spherical, and there is substantial liquid in the walls. In the dry limit, the bubbles become polygonal, and the fluid walls thin. Though based on the description of foam, the concept of wetness is equally applicable to any complex fluid for which a volume fraction, or density, of one of the constituents controls the transition to jamming. Even though there is not a sharp transition from the wet to the dry limit, we will return to the concept of wetness in the context of comparing continuous to discontinuous transitions as a function of applied stress or rate of strain.

The first specific system I will discuss is the bubble raft [15–18, 12]. A bubble raft consists of a single layer of bubbles at the air–water interface. In this regard, it is a quasi-two-dimensional system. The bubbles themselves are still three-dimensional objects. However, the flow is confined to the plane. Careful optical measurements of the bubbles in the raft confirm that there is essentially no motion out of the plane. One also needs to consider the nature of the interaction between the bubbles and the fluid on which it floats. In the Couette experiments, this is minimized by flowing the fluid as well as the bubbles. Since the force between the bubbles and the water is purely viscous, it is proportional to the difference in velocity. Therefore, by flowing the fluid with the bubbles, even though the velocity in the fluid is that of a Newtonian material, it is still closely matched to the velocity of the bubbles. Any viscous drag between bubbles and the underlying water is significantly reduced. In fact, it has been shown that the bubble–bubble interactions completely dominate over any interactions between the bubbles and the fluid below them.

All of the experiments reviewed here use bubbles formed by blowing nitrogen through a solution of 80% deionized water, 15% glycerine, and 5% miracle bubble solution [17]. The measurements are all performed using a Couette style system running under constant rate of strain. In the bubble raft experiments, the outer cylinder is rotated at a constant rate and the inner cylinder is held fixed [17]. When comparing velocity profiles summarized in this paper, it is important to keep this in mind, as many of the other experiments rotate the inner cylinder and hold the outer cylinder fixed. The measured quantity is the azimuthal velocity as a function of the radial position, $v_\theta(r)$, also referred to as the velocity profile. Because the system is essentially two-dimensional, the velocity is measured by tracking the motion of individual bubbles with video images.

A wide range of three-dimensional materials (pastes, slurries, colloids, emulsions, granular matter, and foam[1]) have been studied. Given the wide range of materials, I will not detail the specific characteristics of every system here. For the three-dimensional materials, a more interesting feature is the challenge to develop methods of measuring the velocity profiles, as the materials are fundamentally opaque. Most of the work discussed in this review used magnetic resonance imaging (MRI) techniques that are discussed in detail in [19]. Basically, a pulsed magnetic field method is used to compute the average velocity of the particles in a small sub-volume of the material. Another powerful technique is ultrasonic velocimetry [20]. Briefly, this method uses time-domain cross correlation of ultrasonic speckle patterns. Typically, this involves including tracer particles that are used to produce the speckle pattern. Both the MRI and ultrasonic methods allow for direct measurement of the average velocity profile inside opaque materials. However, in contrast to the bubble raft system, one cannot track the motion of individual bubbles.

Another useful feature of the three-dimensional systems is the ability to compare studies in the Couette geometry and the cone and plate geometry. Using both geometries allows for comparison between homogeneous and inhomogeneous stress. Finally, by using standard rheometers, it was possible for measurements to be made at both constant rate of strain and

[1] One material that is not discussed in detail in this review is granular matter. The reason for this is the focus on discontinuous shear bands. Shear bands are an important topic for granular matter, but most reported examples are for the continuous case in which the velocity varies roughly exponentially (for example, see [37] and [38]). It should be noted that aspects of the discontinuous transition, such as the viscosity bifurcation discussed in section 4, are observed in granular matter [28].

constant stress. The constant stress experiments are especially important in providing detailed information about the source of the discontinuity in the rate of strain that is observed in the constant rate of strain experiments.

Of the wide range of three-dimensional systems that have exhibited a discontinuous jamming transition, it is worth briefly commenting on two systems. One system is a particular colloidal system: spherical poly-(methyl methacrylate) particles with a diameter of 1.4 μm in a solvent consisting of a mixture of cyclohexyl bromide and decalin [11]. An important feature of this system is its optical properties. By appropriate use of matching index of refractions, the motion of individual particles can be tracked using confocal microscopy [21]. The other system is an emulsion of castor oil droplets in water with sodium dodecyl sulfate (SDS) [22]. By varying the amount of SDS in the water, the authors are able to control the nature of the interactions between the emulsion droplets. This provides important insights into the nature of the jamming transition that will be discussed in section 3.

As discussed in the outline, I have selected to include in this review a system that exhibits the coexistence between two *flowing* states. Though not an example of jamming per se, it is very suggestive of a *nonequilibrium* transition between two different fluid phases. Also, the transition is consistent with a discontinuous transition, providing useful insight into general discontinuous, nonequilibrium transitions. The system I have selected to include is worm-like micelles [23]. Micelles are self-assembled structures of surfactant molecules in an aqueous solution. The exact shape of the micelles depends on temperature, concentration of surfactant, etc. Worm-like micelles, as the name implies, are a class of micelles that are elongated and semi-flexible. Another common phase of interest is the lamellar phase, which is composed of sheet of surfactant. The behavior of various phases of micelles is representative of a wide range of materials, including ordered mesophases and transient gels, and their rheological properties have been thoroughly studied (for a review, see [24]). Therefore, it is worth highlighting in this review some of their properties for comparison with the discontinuous jamming transition. For example, these systems are notable for the fact that shear banding is accompanied by well-defined structural changes in the material. They provide an example of an additional useful experimental tool for measuring velocity profiles: dynamic light scattering. The particular study that I will discuss used a solution of cetylpyridinium chloride and sodium salicylate in 0.5 M NaCl brine. The velocity was measured from the interference of a reference laser beam with the scattered light from a roughly 50 μm volume of the material. The interference signal from the two beams exhibits oscillations at a frequency proportional to the local velocity because of the Doppler shift of the scattered beam.

3. Experimental results

3.1. Quasi-two-dimensional system

For the bubble rafts, the key measurement is the velocity profile, i.e. the azimuthal velocity as a function of radial position. Figure 5 illustrates a typical velocity profile for rotation of the outer cylinder. As discussed in section 2.1, the velocity $v(r)$ is the azimuthal velocity $v_\theta(r)$ scaled by Ωr, where Ω is the rotation rate of the outer cylinder. Therefore, regions where $v(r) = 1$ represent rigid body rotation, or jammed states. Also, because the rate of strain, $\dot{\gamma}$, is given by

$$\dot{\gamma} = \frac{1}{r}\frac{\mathrm{d}}{\mathrm{d}r}\left(\frac{v_\theta(r)}{r}\right) = \frac{1}{r}\frac{\mathrm{d}v(r)}{\mathrm{d}r}, \tag{1}$$

a discontinuity in the slope of $v(r)$ is a discontinuity in the rate of strain.

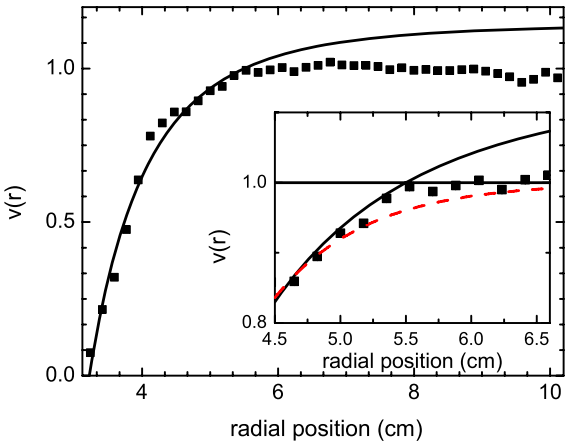

Figure 5. The azimuthal velocity as a function of radial position in a Couette geometry for a bubble raft (solid symbols) (similar velocity profiles are presented in [17] and [12]). The solid line is the velocity profile in this geometry assuming that the stress is proportional to the rate of strain to some power. The insert shows a close up of the transition from flow to no-flow. The discontinuity in the rate of strain is indicated by the velocity curve for the power-law fluid. Also, the case for a fit to an exponential velocity profile is shown for comparison (red dashed line).

The observation of a jammed region is relatively straightforward. From figure 5, the existence of a region with $v(r) = 1$ for all values of r greater than some critical value r_c is apparent. One approach to testing for the existence of a discontinuity in the rate of strain is to fit the velocity profile to various continuum models of materials. In figure 5, the case of a fit to a power-law fluid for the 'flowing region' is given by the solid line. A power-law fluid is one for which the stress is given by the rate of strain to some power ($\sigma = \eta\dot{\gamma}^n$) [10]. A number of examples of continuous shear bands can be well described by an exponential velocity profile. For comparison to the power-law fit, a fit of the velocity profile to an exponential function is given by the dashed line in the insert in figure 5. The insert highlights two facts. First, the exponential fit fails to capture the behavior near the transition from the flowing state to the jammed state. This suggests that the transition is discontinuous. Second, the power-law fit highlights the discontinuity in the rate of strain by providing a clear picture of the slope of $v(r)$ at the transition. As one approaches the critical radius where $v(r) = 1$ from the inner cylinder, the rate of strain (slope of $v(r)$ versus r) is still non-zero. This is the definition of a discontinuous jamming transition, and is the strongest evidence in the bubble rafts for the existence of such

a transition. A more detailed description of the analysis of $v(r)$ is given in [12].

Once it is established that a discontinuous transition exists, one can consider the behavior of the critical rate of strain. The critical rate of strain is the rate of strain measured in the flowing state at the critical radius. For sufficiently large system sizes and rotation rates, there exists a single value of the rate of strain at the transition point [12]. This is what one expects for a system that is well described by continuum mechanics *and* represents the coexistence of two unique states. In this case, a flowing and a solid state. This also allows one to consider the transition to be analogous to a first order phase transition where the jump in density is replaced by a jump in rate of strain.

If the concept of a first order phase transition is to be useful, one should compare the critical rate of strain as measured from velocity profiles to the rate of strain determined directly from stress as a function of the external rate of strain. For a 'phase' transition, one expects that as the external rate of strain is lowered, the stress decreases until the critical rate of strain is reached. At this point, instead of the stress continuing to decrease, the system will separate into regions of flow and no-flow, where the minimum rate of strain in the flow region is the critical rate of strain. The *average* stress remains constant, as part of the system has a zero rate of strain and the other part has the critical rate of strain. The relative sizes of the flowing and jammed states are set by the condition that the applied rate of strain is fixed. This general behavior was illustrated schematically in figure 1.

One challenge with the bubble raft experiments is distinguishing a constant average stress from the behavior of a Herschel–Bulkley model. As discussed in section 1.2, a Herschel–Bulkley model describes the material as having uniform properties (a yield stress and power-law behavior during flow) that by definition result in a continuous variation of the rate of strain. The stress as a function of rate of strain is given by $\sigma = \sigma_y + \eta\dot{\gamma}^n$. Here σ_y is the minimum stress required for flow to occur, and η and n are constants. It turns out that for typical values of n ($n < 1$), the Herschel–Bulkley model exhibits a relatively weak dependence of the stress on the rate of strain at low rates of strain. This is exactly the region in which one expects a constant stress as a function of rate of strain in the phase separation model. This difficulty is illustrated in figure 6. The solid red curve in figure 6 indicates the expected stress behavior in the case of a coexistence between flowing and jammed states with a critical rate of strain. The dashed black line in figure 6 is the case of a Herschel–Bulkley model.

Figure 6 illustrates another challenge of the bubble rafts. Each data point represents a single experimental run. During an individual run, the stress fluctuates due to bubble rearrangements, and each of the points in figure 6 represents the average stress for one of these experimental runs. Each run lasts 20–60 min; the duration being set by when the bubbles pop. For a single run, a steady-state is reached with a well-defined average. (The statistical error in each measurement of the average stress is on the order of the symbol size.) However, it is known that the single runs do not represent a complete exploration of phase space, as the system is trapped in local

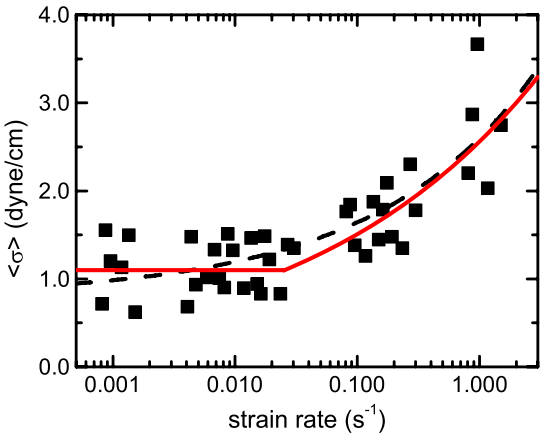

Figure 6. Average stress ($\langle\sigma\rangle$) as a function of the global rate of strain ($\dot{\gamma}$) for a bubble raft in the Couette geometry (similar results are given in [16]). The data are fit to a Herschel–Bulkley model (dashed black curve) and to a power-law fluid that has a critical rate of strain (solid red curve).

regions [25]. The net result is a systematic variation from run to run that is dependent on initial conditions. This leads to variations in the average quantities between runs that are larger than one expects from the statistical error in a single measurement [25]. This is reflected in the fluctuations in the average stress data in figure 6. These fluctuations make it difficult to distinguish the Herschel–Bulkley model from a phase separation picture. Future work will be focused on distinguishing these cases. (Unfortunately, the noise is an intrinsic feature of the bubble rafts at these very slow rates of strain, and represents a significant experimental challenge [16, 25].)

An interesting feature of the bubble rafts is the ability to measure fluctuations around the transition. As we progress in our understanding of the jamming transitions, one expects fluctuations to play an important role. (Again, this is based on our analogy to equilibrium transitions.) Also, even in equilibrium transitions, the question of the exact nature of the interface between two different phases is an open and very interesting question. For example, one of the most basic questions is the instantaneous position of the boundary between flow and no-flow.

Because the instantaneous motion of all the bubbles is measured, one can ask about the location of the transition from flow to no-flow on short timescales. In this case, 'flow' is defined on short timescales by non-affine motion of the bubbles. In other words, because the outer cylinder is rotating, the elastic motion of the bubbles is essentially rigid body rotation. Any deviation from this motion can be interpreted as flow. Therefore, by considering the displacement of bubbles as a function of position and measuring the radial position of the initial deviation from rigid body rotation, the local position of the critical radius can be determined. From this, one can measure statistics such as the width of the critical zone and the time required for the averaging to produce the sharp transition from flow to no-flow. As an initial step [12] reports the distribution of the measured critical radii as a function of the

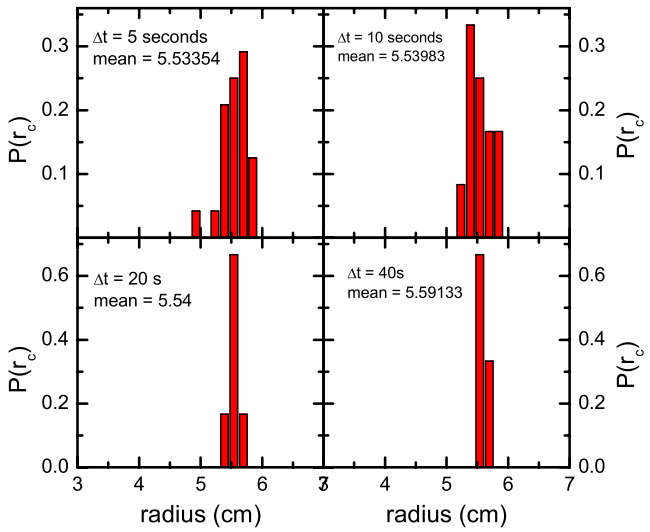

Figure 7. Figure 6 from [12]. Probability distribution of measuring a particular value of the critical radius r_c for the transition from flow to no-flow based on averaging the velocity over finite time intervals. Four different time intervals are illustrated for a rotation rate of the outer cylinder of 0.07 s^{-1}. The time intervals and mean for each distribution are indicated in the figure. Reprinted figure with permission from [12]. Copyright 2006 by the American Physical Society.

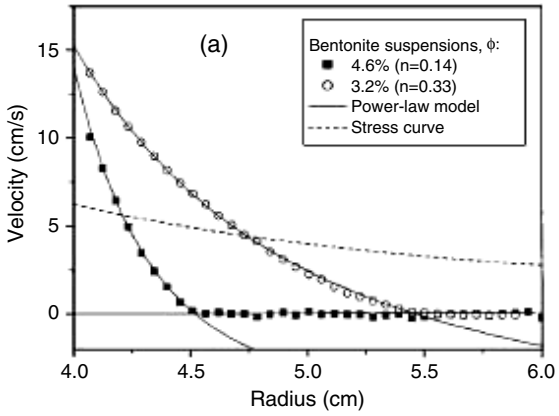

Figure 8. An example of a velocity curve obtained using MRI techniques. This result is taken with permission from [27]. Copyright 2002 by the American Physical Society.

time used to compute the 'flow'. The results are reproduced here in figure 7.

A final question in these systems is the role of the discrete nature of the bubbles. At what point does a continuum model break down, and what happens there? Essentially, once the flowing region is on the order of ten bubbles, one observes the break down of continuum behavior in both this system [12] and three-dimensional foams [26]. The main consequence of this break down is the observation that the critical rate of strain develops a dependence on the external rotation rate and that the width of the flowing region becomes essentially independent of the rotation rate.

3.2. Three-dimensional systems

As with the bubble rafts, one of the main results for the three-dimensional studies is the average velocity profile as a function of the radial position. In [27], a series of materials are studied using MRI techniques for which the discontinuity in the rate of strain is clearly demonstrated. Figure 8 is an example of one of the results from [27]. As with the bubble rafts, one can describe the behavior by fitting the data to the coexistence of a power-law fluid and a solid. This allows for the determination of a critical rate of strain at the transition point. The key element here is the value of the rate of strain, as determined by the power-law fit, in the region of flow, at the point where the transition from flowing to jamming occurs. Visually, this is evident from the continuation of the power-law velocity fit to negative values of the velocity and the slope of the power-law fit at the critical radius. Again, as long as the flowing region is large enough, a single critical rate of strain is determined as a function of external rotation rate.

For the three-dimensional experiments, constant stress experiments have been carried out using standard rheometers [28–30]. For a traditional yield stress fluid, one would expect that if the applied stress is below the yield stress, the material would initially deform by some amount (the elastic response), but it would eventually stop deforming and the rate of strain would go to zero. As the stress is increased above the yield stress, the material would flow, with the rate of strain increasing continuously from zero. Instead, in the experiments one observes a jump in the rate of strain from zero to a non-zero value [28, 29]. This is illustrated by the left-hand panel of figure 9. For low values of applied stress, the viscosity diverges as a function of time. Because viscosity η is given by $\eta = \sigma/\dot{\gamma}$, this indicates an elastic material in which $\dot{\gamma}$ goes to zero. For a continuous transition, when the applied stress is above the yield stress, $\dot{\gamma}$ would increase continuously from zero, and one would observe a continuous variation in the steady-state value of η. Instead, above an applied stress of 3 Pa, there is a large jump in the late-time value of η, indicating a discontinuous jump in $\dot{\gamma}$. This is perhaps the most straightforward evidence for the discontinuity in the rate of strain at the onset of flow.

Another picture of the discontinuity is illustrated in the right-hand panel of figure 9. This figure includes data from constant rate of strain experiments, for which one expects behavior as was discussed in the context of figure 6. Briefly, as the rate of strain is decreased, there is a critical value below which the average stress is constant. This is illustrated by the diamonds in figure 9. For comparison, the stress as a function of rate of strain as determined by the constant stress measurements are represented in figure 9 by the open squares. This data is taken directly from the left-hand panel of figure 9, and by definition, only exists above the critical rate of strain. If the discontinuous phase transition picture is accurate, the two values of the critical rate of strain (one obtained from constant applied stress and one from constant applied rate of strain) should agree. In the context of the right-hand panel of figure 9, this translates into the fact that the plateau region for average stress at low rates of strain begins at the same value of rate of strain at which the constant stress data ends. It is worth comparing the right-hand panel of figure 9 to the results for the

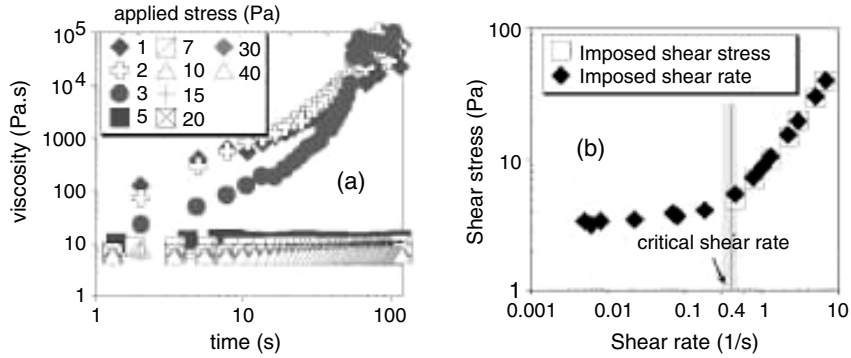

Figure 9. Figure 1 from [29]. This figure illustrates both the jump in the rate of strain (as measured by the viscosity) under conditions of constant stress (left-hand panel) and the behavior of the average stress as a function of applied rate of strain when a critical rate of strain exists (right-hand panel). Reprinted figure with permission from [29]. Copyright 2005 by the American Physical Society.

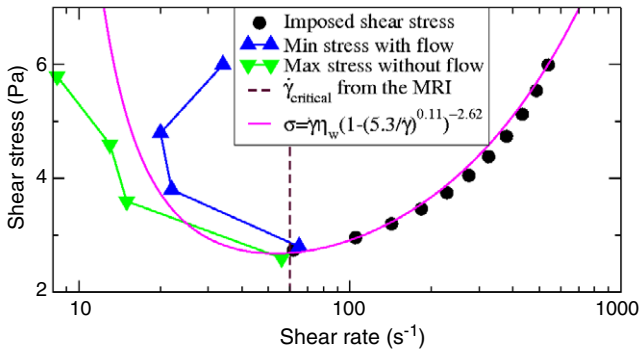

Figure 10. Figure 4 from [30]. Illustrates the measurement of the unstable branch of the stress versus rate of strain curve. The solid line is the prediction of the model proposed in [30] to explain the critical rate of strain. The symbols are data taken under various conditions. Reprinted figure with permission from [30]. Copyright 2008 by the American Physical Society.

bubble raft (figure 6). In the larger three-dimensional system, one does not have the same degree of variation in the average stress between runs. Therefore, it is easier to distinguish a constant stress as a function of applied rate of strain from other cases.

Additional evidence for the discontinuous jamming transition is obtained by considering the flow in the cone and plate geometry [27, 30]. In this case, the stress is now uniform across the system. Therefore, if the material is exhibiting shear banding because it possesses a yield stress and the stress is inhomogeneous, shear banding should not be observed in this geometry. In fact, shear banding is observed with the MRI experiments, providing additional evidence for the phase coexistence picture.

Finally, as will be discussed in section 4, a key element of many models of shear banding is a region of the stress as a function of rate of strain curve for which the slope is negative. This represents a region of unstable flow, so it cannot be observed in steady-state. However, the system can be prepared near this branch with a fixed applied stress. If the initial rate of strain is less than the value of the unstable branch, the rate of strain will continue to decrease. If it is greater than the unstable branch, it will increase. By locating the transition from decreasing to increasing rates of strain under a fixed applied stress, one can determine the location of the unstable branch. This has been accomplished for at least one colloidal system (see figure 4 from [30], reproduced here as figure 10).

In figure 10, the evidence for an unstable flow curve is presented. To the right of the vertical dashed line (high rates of strain), there is a well-defined rate of strain for each value of the applied stress. This represents the stable branch of the flow curve. To the left of the dashed line, there are two experimental curves. These are determined by starting in a wide range of initial states with various pairings of stress and rate of strain. If under fixed stress the system slows down/speeds up, it is to the left/right of the unstable branch. The down triangles represent the maximum applied stress that results in the system slowing down and the up triangles are the minimum stress that results in a speeding up of the flow. The unstable branch is located between these two values. The solid line is the prediction of the stress versus rate of strain curve from a model discussed in [30].

An important step in our understanding of the nature of discontinuous versus continuous transitions is reported in [22]. As described in section 2, measurements were made of the velocity profiles for emulsions under varying conditions of attraction. The key result was the observation of a discontinuous jamming transition for adhesive emulsions and the observation of homogeneous flow for non-adhesive emulsions. This suggests an important direction for future theoretical studies of the jamming transition.

Another important experiment in terms of providing guidance for the modeling of the discontinuous jamming transition is the work with the colloidal system described in detail in section 2 [11]. In this case, one observes a critical frequency at which fluid and solid-like behavior coexist. As with the other experiments, the coexistence point moves as a function of the applied frequency. An example of the behavior reported in [11] is given in figure 11. Here the solid lines are fits to the displacement data. The kink between the two lines is the location of the rate of strain discontinuity. The main difference between this system and the other systems is the fact that the fluid state in this case is Newtonian.

One consequence of the fact that the fluid-like phase is Newtonian is that this transition is definitely not the result

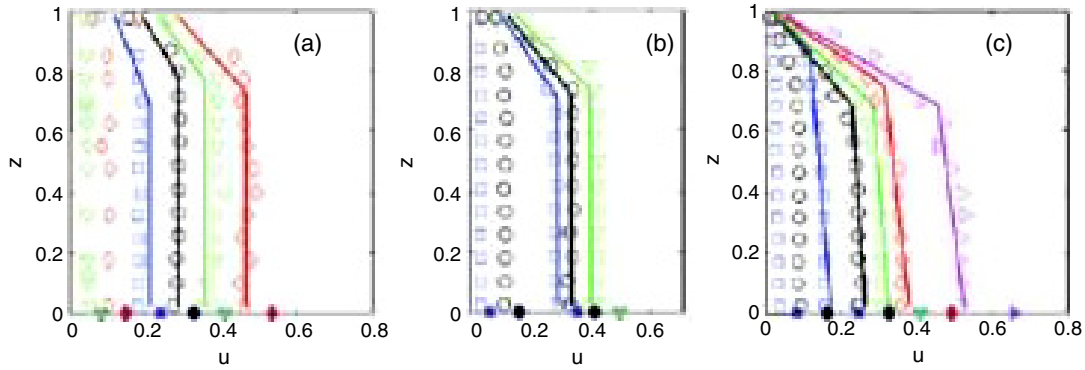

Figure 11. An excerpt from figure 1 from [11]. Illustrated here is the flow profiles for various applied frequencies as a function of the position (z) in the system. The profiles are given by the maximal displacement of the particles (u). Reprinted with permission from [11]. Copyright 2006 by the American Physical Society.

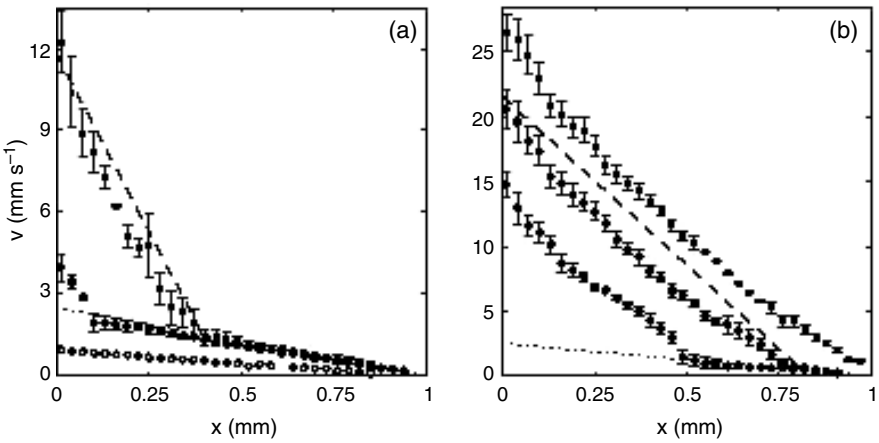

Figure 12. Figure 2 from [23] illustrating the discontinuity in the velocity profile in worm-like micelles. Reprinted figure with permission from [23]. Copyright 2003 by the American Physical Society.

of the material being a yield stress fluid. There is still the equivalent of a 'yield stress' for the system in the sense that there is a value of the stress which determines when the solid switches to a fluid. However, the description used to interpret the results requires a two phase model for the material, but no nonlinearity is needed in the stress-rate of strain relation.

3.3. Micelles

A brief discussion of the worm-like micelle system is included as an important additional example of a shear band with a *discontinuous* change in the rate of strain. In this case, the system exhibits behavior that is a classic example of phase coexistence [23]. In a standard imposed rate of strain experiment, the system reaches a stress plateau. At this point, local velocity measurements establish the existence of two distinct flow regimes in the material. The two regimes are characterized by different rates of strain. Because of the geometry used to generate flow, the velocity profiles are linear. Therefore, the slope of the velocity versus position curve is the rate of strain. In figure 12, the solid lines represent the fits to the velocity. Where they meet at a kink is the location of the discontinuity in the rate of strain. If the experiments are carried out as a function of increasing the applied rate of strain, the region with a higher rate of strain increases in size until it fills the system. At this point, the measured stress increases again. Measurements of the material reveal distinct microstructures in the two flow regimes, consistent with a phase transition picture. A typical result from [23] is reproduced here in figure 12. It is worth noting that shear banding has also been observed in lamellar phases [31].

The worm-like micelle and lamellar systems are interesting for an additional reason. As with the bubble raft system, studies of the dynamics of the interface between the two flow regimes have been carried out [32, 33]. As mentioned in the discussion of bubble rafts, detailed measurements of the dynamics of the interface at a rate of strain discontinuity promise to provide additional insight into this phenomenon.

4. Modeling the rate of strain discontinuity

The focus of this review is the experimental studies of the discontinuous jamming transition; therefore, this section is not intended to be a detailed discussion of the various models that have been proposed to describe the behavior. Instead, I will provide a brief overview of some of the essential features of

various models. One motivation for this is the fact that the experimental evidence for a discontinuous transition in many different systems is well established; however, though many general features of how to model this behavior have emerged, the theoretical picture at this time is not as well established.

Once one accepts the general concept of a phase coexistence, one expects a situation in which there are at least two values of the rate of strain (zero and the critical rate of strain) for a single value of the stress. (Recall, that this is depicted schematically in figure 1, and experimental results are illustrated by figures 6, 9, and 10.) When this occurs, at fixed rate of strain, the system must 'phase separate' to these two different values. The amount of each phase is determined by a standard application of the Lever rule. Though a number of models propose more complicated stress versus rate of strain curves, for example, with regions of stress increasing as the rate of strain decreases (see for example, [30]), to explain the data, this simple picture captures the essence of those explanations.

One of the more developed concepts that is able to explain a range of discontinuous transitions is viscosity bifurcation. This concept has been developed in a series of papers [28–30]. The model is based on the experimental observation illustrated in the left-hand panel of figure 9. Under conditions of constant stress, a wide range of materials have been shown to exhibit a jump in the viscosity as a function of applied stress. This is the phenomenon that viscosity bifurcation describes. Taking the general context of a viscosity bifurcation as the starting point, various models have been proposed to explain this phenomenon in specific systems.

Early work focused on three experimental systems [28]: granular matter, foams, and emulsions. In this case, the modeling of the viscosity bifurcation focused on the granular system. By making an analogy to the dynamics of a single grain on a plane [34], the authors proposed a simple model for the flow. Two essential ingredients were a velocity dependent force to describe the trapping of particles (F_0) and a velocity dependent force describing steady motion (F_∞). A velocity dependent function h was used as a matching function, with the total force given by $F = (1-h)F_\infty$. The dynamics were given by $F = \mathrm{d}V/\mathrm{d}t$. Simulations showed that this simple model was enough to reproduce the viscosity curves and the existence of a viscosity bifurcation [28].

Additional work on the viscosity bifurcation involved dense pastes [29]. (This is the work in which figure 9 appeared.) In this case, a different, material specific, model was used to describe the viscosity bifurcation. For the dense paste, there are basically two regimes: frictional and lubrication flow. The dimensional parameter that describes the competition between lubrication and frictional forces is the Leighton number $Le = \eta_s\dot{\gamma}/\sigma$, where η_s is the viscosity of the interstitial fluid. It was found that the critical rate of strain at which the viscosity bifurcation occurred was set by the Leighton number [29].

More recently, the case of a colloidal system has been considered [30]. In this case, a microscopic model has been proposed based on three elements in the system. First, aging in the system leads to the development of clusters of colloidal particles that grow in time. Second, it is the size of these clusters, and not the particle diameter, that is the important length scale in determining the rheological response of the material. And finally, an applied rate of strain breaks up these clusters. The timescales for the formation and break up of the clusters are different. Combining these factors results in a stress as a function of rate of strain illustrated in figure 10. Therefore, this model captures the existence of the critical rate of strain that is essential to the viscosity bifurcation. Additionally, it predicts a region of negative slope in the stress as a function of rate of strain curve (see figure 10 and [30]). Given this prediction, the experimental confirmation of the region of negative slope represents an important step in our understanding of discontinuous jamming transitions [30].

The three models used to describe the viscosity bifurcation in three different systems all involve the competition between two dynamical processes in the system. This suggests that looking for such a competition in other systems will be useful. However, the microscopic details appear to be rather varied between the three systems. For example, the model for the colloidal system discussed in [30] is based on a microscopic picture in terms of spatial structures in the material. This should be contrasted to the explanations based on a competition between forces with little or no structural change occurring in the system.

In the context of the experiments reviewed in this paper, it is worth comparing this detailed model of the viscosity bifurcation in a particular colloidal system with that proposed as an explanation for the results of the oscillatory experiments [11]. The apparent difference is whether or not a nonlinear stress-rate of strain relation is needed. In the case of the oscillatory experiments, the data is well described by the coexistence of a Newtonian fluid and an elastic solid. However, this is not a contradiction with the explanation for the viscosity bifurcation for the colloidal system proposed in [30]. Instead, one can view it as a special case in which the unstable branch reduces to a single point, the yield stress. This arises naturally in the details of the proposed model for how the colloidal particles cluster [30].

Finally, it is worth returning to the possible impact of the 'wetness' of the material and commenting on a different approach to the question of shear bands that is based on experiments with very dry foams. In this case, the shear banding is proposed to be the result of a dynamical focusing of the stress fields [35]. As discussed, the fundamental element of flow in foams is a T1 event in which bubbles switch neighbors. Modeling of this process suggests that T1 events can act to focus stress in such a fashion as to lead to shear banding. In contrast to the models and experiments already discussed in this paper, this model produces a continuous transition in that the rate of strain decays exponentially. However, the decay length can be of the order of a single bubble, and it has been suggested that this behavior could account for discontinuous shear bands in which the discontinuity has not been resolved at the level of single bubbles, or particles [36]. In considering this proposal, it is worth reiterating the following aspects of the experiments reviewed in this paper.

First, even though the measurements of the shear bands using MRI do not have single particle resolution, the constant

stress measurements strongly support a true discontinuity in the rate of strain [29]. Second, the two-dimensional bubble raft measurements [12] and the confocal velocity measurements in the oscillating shear experiment [11] do have a resolution at the single particle level. Therefore, there is extremely strong evidence for the discontinuity even at the single particle level, and it is unlikely that the stress focusing model, as proposed, can account for the discontinuous shear banding. However, I include it in this review as this points to an important direction for future research.

It is not sufficient to explain the source of discontinuous jamming transitions; one also wants to understand why some transitions are continuous and others are discontinuous. A common feature of the experimental systems reviewed in this paper is that they can be considered to be in the relatively 'wet' limit. Again, there is no precise definition of this at the current time. But, the dynamical model based on T1 events is definitely applicable to a dry foam, in which the dynamics of the films, and not the bubbles, dominates [13]. Therefore, an important question for future research is developing a workable definition of wetness and determining if this acts as a control parameter for the transition from continuous to discontinuous transitions. Returning to the analogy with equilibrium transitions, as with the gas–liquid transition, one might reasonably expect there to exist the equivalent of a well-defined critical point at which the transition switches from continuous to discontinuous. Another important direction to consider is the connection, if any, between 'wetness' and the results with adhesive emulsions [22].

5. Summary

I have reviewed a diverse set of experiments that demonstrate strong evidence for the existence of a discontinuous jamming phase transition. One consequence of such a transition is the existence of shear bands with a discontinuity in the rate of strain. In the case of a constant applied rate of strain, this results in behavior reminiscent of a classic first order phase transition in which the measured stress is constant for a range of applied rates of strain. In this range, the system divides into two distinct regimes with different rates of strain, which on average, correspond to the fixed applied rate of strain. An exciting feature of this behavior is the relatively wide range of systems in which it is observed, including both three-dimensional and quasi-two-dimensional systems.

A generic picture is presented for understanding the existence of discontinuous jamming transitions: the existence of an unstable branch in the stress-rate of strain relation. As an example, a specific model for a viscosity bifurcation based on the competition between the applied shear and aging in the system is reviewed. In this case, the shear breaks up clusters of the material as the aging increases cluster sizes. This competition results in a model of the stress as a function of rate of strain that has a critical rate of strain. Essentially, the existence of a critical rate of strain can be understood in terms of the competition between rates for the two different processes in the system. Having this physical picture for one system, it is interesting to ask about the application to other very different systems, such as the bubble rafts. In the bubble rafts, there has been no observation of aging at this point, but this does not rule out other similar competition of timescales. Despite the existence of a number of promising models, there are many open theoretical questions. For example, the issue of predicting whether or not a particular jamming transition is continuous or discontinuous is raised.

In conclusion, we are at an exciting point in the study of the jamming transition. There is sufficient experimental evidence to take seriously the existence of a discontinuous jamming transition. However, there are still a number of open questions that require both additional theoretical and experimental efforts.

Acknowledgments

There are many people who have provided insights and exciting discussions of the jamming transition. I would like to thank A Liu and D Durian for introducing me to this exciting field and for all of their discussions. I would like to thank P Coussot and D Bonn for their discussions of the three-dimensional systems and the connections with the bubble raft. I would like to thank K Krishan for his discussions of the manuscript and jamming in general. Finally, I would like to thank all the authors that were willing to allow use of their figures in this review.

References

[1] Cates M E, Wittmer J P, Bouchaud J-P and Claudin P 1998 *Phys. Rev. Lett.* **81** 1841
[2] Liu A J and Nagel S R 1998 *Nature* **396** 21
[3] Liu A J and Nagel S R (ed) 2001 *Jamming and Rheology* (London: Taylor and Francis)
[4] Two examples are Bird R B, Armstrong R C and Hassage O 1977 *Dynamics of Polymer Liquids* (New York: Wiley)
Macosko C 1994 *Rheology Principles, Measurements, and Applications* (New York: VCH)
[5] Sollich P, Lequeux F, Hébraud P and Cates M E 1997 *Phys. Rev. Lett.* **78** 2020
[6] Sollich P 1998 *Phys. Rev.* E **58** 738
[7] Falk M L and Langer J S 1998 Dynamics of viscoplastic deformation in amorphous solids *Phys. Rev.* E **57** 7192–205
[8] Trappe V, Prasad V, Cipelletti L, Segre P N and Weitz D A 2001 *Nature* **411** 772
[9] Moller P C F, Mewis J and Bonn D 2006 *Soft Matter* **2** 274
[10] Bird R B, Armstrong R C and Hassager O 1977 *Dynamics of Polymer Liquids* (New York: Wiley)
[11] Cohen I, Davidovitch B, Schofield A B, Brenner M P and Weitz D A 2006 *Phys. Rev. Lett.* **90** 215502
[12] Gilbreth C, Sullivan S and Dennin M 2006 *Phys. Rev.* E **74** 051406
[13] Weaire D and Hutzler S 1999 *The Physics of Foams* (Oxford: Claredon)
[14] O'Hern C S, Silbert L E, Liu A J and Nagel S R 2003 Jamming at zero temperature and zero applied stress: the epitome of disorder *Phys. Rev.* E **68** 011306
[15] Bragg L and Lomer W M 1949 *Proc. R. Soc.* A **196** 171
[16] Pratt E and Dennin M 2003 *Phys. Rev.* E **67** 051402
[17] Lauridsen J, Chanan G and Dennin M 2004 *Phys. Rev. Lett.* **93** 018303

[18] Dennin M 2004 *Phys. Rev.* E **70** 041406
[19] Raynaud J S, Moucheront P, Baudez J C, Bertrand F, Guilbaud J P and Coussot P 2002 *J. Rheol.* **46** 709
[20] Manneville S, Bécu L and Colin A 2004 *Eur. Phys. J. Appl. Phys.* **28** 361
[21] Weeks E R, Crocker J C, Levit A C, Schofield A and Weitz D A 2000 Three-dimensional direct imaging of structural relaxation near the colloidal glass transition *Science* **287** 627
[22] Bécu L, Manneville S and Colin A 2006 *Phys. Rev. Lett.* **96** 138302
[23] Salmon J-B, Colin A, Manneville S and Molino F 2003 *Phys. Rev. Lett.* **90** 228303
[24] Berret J-F 2005 *Molecular Gels* (Dordrecht: Springer) pp 235–75
[25] Wang Y, Krishan K and Dennin M 2007 *Phys. Rev. Lett.* **98** 220602
[26] Rodts S, Baudez J C and Coussot P 2005 *Europhys. Lett.* **69** 636
[27] Coussot P, Raynaud J S, Bertrand F, Moucheront P, Guilbaud J P, Huynh H T, Jarny S and Lesueur D 2002 *Phys. Rev. Lett.* **88** 218301
[28] DaCruz F, Chevoir F, Bonn D and Coussot P 2002 *Phys. Rev.* E **66** 051305
[29] Huang N, Ovarlez G, Bertrand F, Rodts S, Coussot P and Bonn D 2005 *Phys. Rev. Lett.* **94** 028301
[30] Moller P C F, Rodts S, Michael M A J and Bonn D 2008 *Phys. Rev.* E **77** 041507
[31] Salmon J-B, Manneville S and Colin A 2003 Shear banding in a lyotropic lamellar phase. i. Time-averaged velocity profiles *Phys. Rev.* E **68** 051503
[32] Salmon J-B, Manneville S and Colin A 2003 Shear banding in a lyotropic lamellar phase. ii. Temporal fluctuations *Phys. Rev.* E **68** 051504
[33] Lerouge S, Argentina M and Decruppe J P 2006 Interface instability in shear-banding flow *Phys. Rev. Lett.* **96** 088301
[34] Quartier L, Andreotti B, Douady S and Daerr A 2000 *Phys. Rev.* E **62** 8299
[35] Kabla A and Debrégeas G 2003 *Phys. Rev. Lett.* **90** 258303
[36] Kabla A, Scheibert J and Debrégeas G 2007 *J. Fluid Mech.* **587** 45
[37] Bocquet L, Losert W, Schalk D, Lubensky T C and Gollub J P 2001 *Phys. Rev.* E **65** 011307
[38] Howell D, Behringer R P and Veje C 1999 *Phys. Rev. Lett.* **82** 5241